# Characterization of the Conformational Changes of Acetohydroxy Acid Isomeroreductase Induced by the Binding of $Mg^{2+}$ Ions, NADPH, and a Competitive Inhibitor†

Frédéric Halgand,‡ Renaud Dumas,*,§ Valérie Biou,‡ Jean-Pierre Andrieu,‡ Karine Thomazeau,‡ Jean Gagnon,‡ Roland Douce,§ and Eric Forest*,‡

*Institut de Biologie Structurale, CEA/CNRS, 41 Avenue des Martyrs, 38027 Grenoble Cedex, France, and Unité Mixte CNRS/Rhône-Poulenc, 14-20 Rue Pierre Baizet, 69263 Lyon Cedex 09, France*

*Received October 9, 1998; Revised Manuscript Received January 29, 1999*

ABSTRACT: Acetohydroxy acid isomeroreductase (EC 1.1.1.86), the second enzyme of the parallel branched chain amino acid pathway, is a homodimer with an $M_r$ of ≈114000 which in the presence of $Mg^{2+}$ ions catalyzes an unusual alkyl migration followed by an NADPH-dependent reduction. Prior binding of NADPH and $Mg^{2+}$ to the enzyme was shown to be required for substrate or competitive inhibitor [*N*-hydroxy-*N*-isopropyloxamate (IpOHA)] binding [Dumas, R., et al. (1994) *Biochem. J. 301*, 813−820]. Moreover, crystallographic data for the enzyme−NADPH−$Mg^{2+}$−IpOHA complex [Biou, V., et al. (1997) *EMBO J. 16*, 3405−3415] have shown that IpOHA was completely buried inside the active site. These observations raised the question of how the reaction intermediate analogue inhibitor can reach the active site and implied that conformational changes occurred during the binding process. With a view of characterizing these conformational changes, H−D exchange experiments combined with mass spectrometry were performed. Results demonstrated that $Mg^{2+}$ ions and NADPH binding led to an initial conformational change at the interface of the two domains of each monomer. Binding of the two cofactors to isomeroreductase alters the structure of the active site to promote inhibitor (substrate) binding, in agreement with the ordered mechanism of the enzyme. Structural changes remote from the active site were also found. They were interpreted as long-range structural effects on the two domains and on the two monomers in the time course of the ligand binding process.

Acetohydroxy acid isomeroreductase (EC 1.1.1.86, isomeroreductase, Ir[1]), which is the second enzyme of the parallel branched chain amino acid pathway, has been the subject of extensive biochemical and crystallographic studies (*1*, *2*). The plant enzyme is a homodimer with an $M_r$ of ≈114000, which catalyzes a $Mg^{2+}$-dependent two-step reaction in which the substrate, either 2-acetolactate or 2-aceto-2-hydroxybutyrate (AHB), is converted via an alkyl migration and a NADPH-dependent reduction to yield 2,3-dihydroxy-3-isovalerate (synthesis of valine and leucine) or 2,3-dihydroxy-3-methylvalerate (synthesis of isoleucine), respectively (*3*).

To obtain more information on this enzyme, the gene encoding the mature polypeptide of isomeroreductase from spinach leaf chloroplasts has been used to transform *Escherichia coli* strains to produce large amounts of the plant isomeroreductase (*3*). Kinetic studies have shown that isomeroreductase obeys an ordered mechanism in which NADPH and $Mg^{2+}$ ions bind first and independently, followed by acetohydroxy acid substrate binding (*3*). These results are in agreement with those reported for the corresponding enzymes isolated from *E. coli* (*4*).

A decrease in the emitted fluorescence of the enzyme−NADPH binary complex upon addition of $Mg^{2+}$ ions has suggested that binding of this metal ion may trigger some conformational modifications. Furthermore, the emitted fluorescence of the enzyme−NADPH−$Mg^{2+}$ ternary complex was also greatly modified upon addition of a transition state analogue, *N*-hydroxy-*N*-isopropyloxamate (IpOHA), indicating that binding of the inhibitor to the active site leads to further conformational changes (*5*).

Alignment of the predicted amino acid sequence of acetohydroxy acid isomeroreductase from plants, fungi, and bacteria revealed five conserved regions designated I−V (*2*). The conserved residues cluster closely around the active site in the three-dimensional structure (*1*). Alignment with other reductases showed that region I is involved in NADPH binding (*6*). Steady state kinetic analyses and fluorescence experiments with the mutants of regions III and IV indicated that each of these domains was implicated in the binding of

† This study has been conducted under the BIO AVENIR program financed by Rhône-Poulenc with the contribution of the Ministère de la Recherche et de l'Espace and the Ministère de l'Industrie et du Commerce Extérieur. The CEA is also acknowledged for the cofinancing of the grant to F.H.

* Authors to whom correspondence should be addressed. E.F.: telephone, + (33) 4 76 88 34 03; fax, + (33) 4 76 88 54 94; e-mail, eric.forest@ibs.fr. R.D.: telephone, + (33) 4 72 85 22 96; fax, +(33) 4 72 85 22 97; e-mail, renaud.dumas@ladargoire.rhone-poulenc.com.

‡ CEA/CNRS.

§ Unité Mixte CNRS/Rhône-Poulenc.

[1] Abbreviations: Ir, acetohydroxy acid isomeroreductase or isomeroreductase; A, α-helix; B, β-strand; ESI, electrospray ionization; H−D exchange, hydrogen−deuterium exchange; MS, mass spectrometry; $Mg^{2+}$ 1, $Mg^{2+}$ ion which binds on region III; $Mg^{2+}$ 2, $Mg^{2+}$ ion which binds on regions III and IV.

10.1021/bi982412e CCC: $18.00 
Published on Web 04/20/1999

two $Mg^{2+}$ ions, $Mg^{2+}$ 1 and $Mg^{2+}$ 2, involved in the isomerization and reduction reaction (*2*). More recently, X-ray crystallographic data obtained for the Ir−NADPH−$Mg^{2+}$−IpOHA complex, at 1.65 Å resolution, have confirmed that region I is the binding site of NADPH and showed that region II is involved in NADPH stabilization on the dinucleotide binding loop. Furthermore, the interactions with the two $Mg^{2+}$ ions were more precisely defined. Thus, $Mg^{2+}$ 1 was found to bind only on region III, whereas $Mg^{2+}$ 2 binds both on region III and on region IV via water molecules. Region V was shown to take part in the active site, interacting with the carboxylate group of the competitive inhibitor (*1*).

Crystallographic results also showed that the native enzyme is a homodimer, in which each monomer consists of two domains: the N-terminal domain with a NADPH binding site and the C-terminal domain involved in the binding of the competitive inhibitor and two $Mg^{2+}$ ions. The C-terminal domain alone is involved in dimer formation with structurally important α-helices A17 and A18 and a loop (residues 422−432) called the dimer loop (see Figure 1A) forming the interface. Indeed, mutagenesis studies (*7*) have shown that deletion of the dimer loop generates an active monomer. Moreover, the two $Mg^{2+}$ ions interact strongly with IpOHA via an important electrostatic interaction network, leading to extensive binding of the inhibitor in the active site. Thus, in this complex, the inhibitor is completely buried inside the active site at the interface of the two domains. This observation raised the question of how IpOHA can reach the active site and implied that conformational modifications occurred during the binding process.

The advent of the soft ionization method electrospray ionization (ESI) has enabled the detection of intact peptides and proteins in aqueous media by mass spectrometry. The demonstrated relationship between the charge state distribution of the electrospray ionization spectra and the state of the protein in aqueous solution allows the use of this technique in studying the conformational influence of several physical and chemical factors on protein structure (*8*). This technique allows the determination of the accurate mass of peptides and proteins with a typical error of 0.01%. On the basis of this accuracy, ESI-MS has proven to be suitable for the study of hydrogen−deuterium (H−D) exchange (*8*). The combination of H−D exchange and ESI-MS was demonstrated to be a useful tool for obtaining structural information about proteins (*9*). The measurement of the rate of H−D exchange has provided considerable insight on peptide (*10*) and protein (*11*) stability and dynamics (*12*), for example, in the study of protein folding (*13*) and protein−protein interactions (*14*−*16*). Hydrogen exchange studies have also been used to identify protein segments influenced by mutation (*17*) or by the binding of a ligand (*18*, *19*). The main advantages of the combination of H−D exchange with ESI-MS, compared to NMR or X-ray cristallography, lie in the relatively low amount of biological material that is required and the ability to study large proteins. This technique is therefore well suited to probing the effects of low-molecular mass ligands on large proteins with a molecular mass of greater than 100 kDa.

With a view of obtaining conformational information about the binding of the $Mg^{2+}$ ions, NADPH, and a competitive inhibitor (IpOHA), we carried out ESI-MS experiments using isotopic exchange on isomeroreductase. The data that were collected provided precise information about the dynamics of the ligand binding process.

## MATERIALS AND METHODS

### *Materials*

Polypropylene glycol and magnesium chloride were purchased from Aldrich. Deuterated water and the reduced form of NADPH were purchased from Sigma. Pepsin immobilized on agarose gel was purchased from Pierce. The gene encoding the mature acetohydroxy acid isomeroreductase from spinach chloroplasts was used to transform *E. coli* strains and to overexpress the enzyme (*3*).

### *Methods*

*ESI-MS Analyses.* Mass spectra were obtained using a Sciex API III+ triple-quadrupole mass spectrometer (Perkin-Elmer Sciex) equipped with a nebulizer-assisted electrospray (ionspray) source. The instrument was calibrated using polypropylene glycol. The ionspray voltage was set at 5 kV, and the orifice voltage was 60 V for peptide analyses. For calculation of peptide masses prior to Edman degradation analyses, mass spectra were recorded from *m*/*z* 400 to 1400 in steps of 0.5 *m*/*z* with a 2 ms dwell time per step. For analysis of deuterated peptides, mass spectra were recorded from *m*/*z* 400 to 1400 in steps of 0.2 *m*/*z* with a 1 ms dwell time per step. The nebulizer gas was nitrogen to prevent back exchange during the ionization-desorption process. Mass spectra were acquired using a Quadra 950 data system (Apple), and molecular masses were calculated using MacSpec software (Perkin-Elmer Sciex).

*Preparation of the Enzymatic Complexes.* The enzyme−ligand complexes (Ir−$Mg^{2+}$, Ir−NADPH, Ir−$Mg^{2+}$−NADPH, and Ir−$Mg^{2+}$−NADPH−IpOHA) were obtained by sequential addition of $Mg^{2+}$ ions, NADPH, and IpOHA in a 1:5 ratio, with respect to the enzyme. The complexes were formed in the standard Hepes buffer (15 mM, pH 7.5) of isomeroreductase and incubated for 35 min at room temperature, prior to addition of $D_2O$ for H−D exchange.

*H−D Exchange Experiments with Peptides.* Three nanomoles of free isomeroreductase or isomeroreductase complexed with ligands was dissolved in $D_2O$ to a final volume of 50 μL and the mixture incubated for 3 h at 30 °C, under nitrogen at pD 7.7 to exchange all accessible amide hydrogens for deuterium. Pepsin immobilized on agarose gel (300 μL) was deposited into an ultrafree Mc filter cup (Millipore) with a 30 kDa cutoff and extensively washed with HCl at pH 2.2 to avoid all possible contamination. Afterward, immobilized pepsin was dried by high-speed centrifugation and precooled in an ice bath before the next step was undertaken. Back exchange was quenched by addition of 150 μL of precooled HCl at pH 2.2 to the deuterated protein sample, and the final solution was mixed with immobilized pepsin. Digestion occurred rapidly in 5 min at 0 °C, while the mixture was magnetically stirred, with an enzyme:substrate ratio of 3:1 (w:w). Peptic fragments were removed from the agarose gel by centrifugation at 12000*g* for 2 min and rapidly separated on a $C_8$ Brownlee (2.1 mm × 100 mm) column using a linear gradient from 16 to 40% acetonitrile over the course of 7 min at a flow

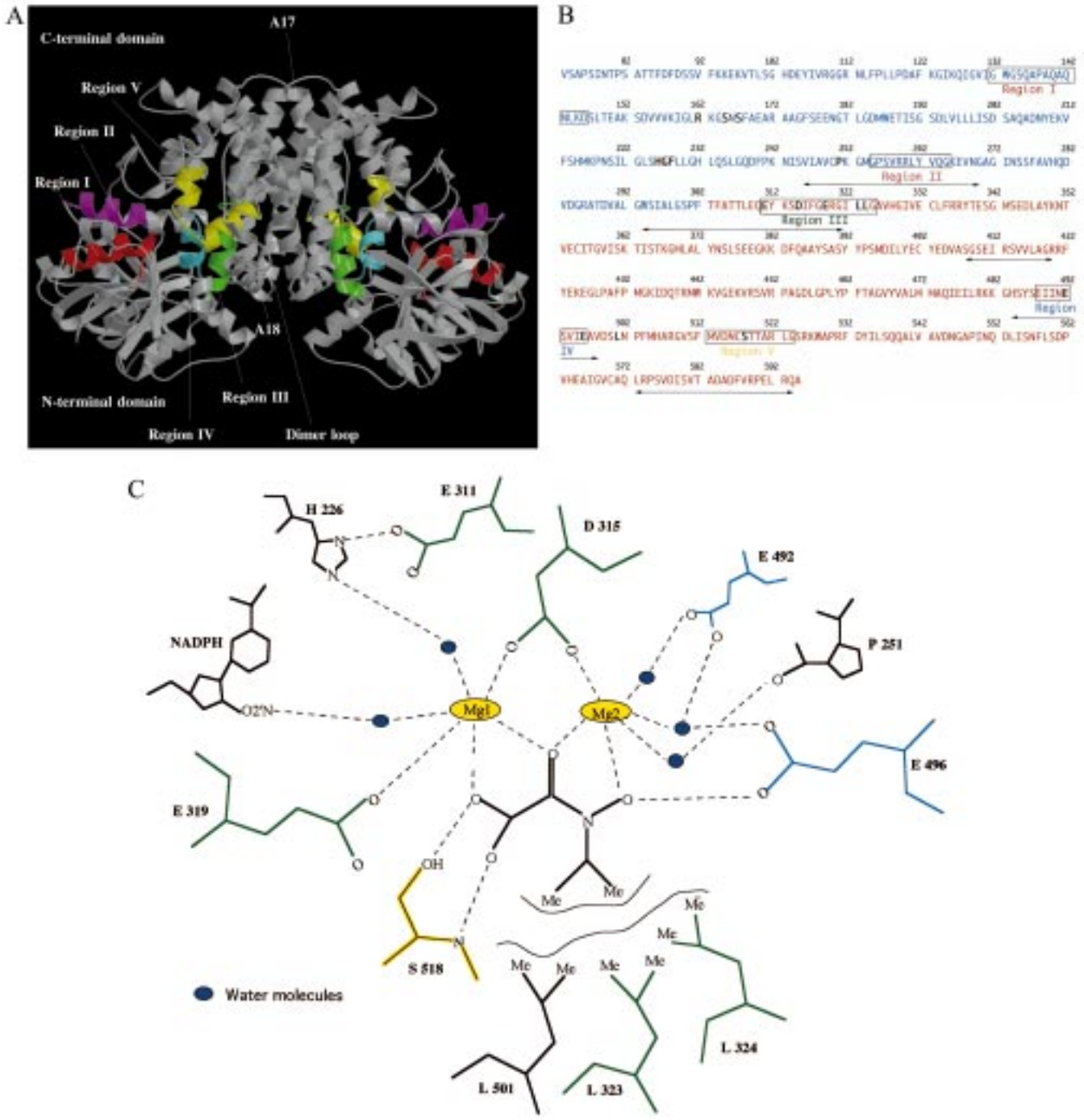


FIGURE 1: Details of selected secondary structures of isomeroreductase. (A) Crystallographic structure of the acetohydroxy acid isomeroreductase complexed with NADPH−$Mg^{2+}$−IpOHA (*1*). Region I (red) corresponds to the binding site of NADPH. Region II (purple) corresponds to the region interacting with region I for NADPH stabilization. Region III (green) is the binding site of $Mg^{2+}$ 1. Region IV (cyan) is the binding site of $Mg^{2+}$ 2. Region V (yellow) contains conserved amino acids of the active site. Mentioned secondary structures A17, A18, and the dimer loop that extends out toward the other monomer are responsible for dimer contacts. (B) The sequence of acetohydroxy acid isomeroreductase shows regions at the interface of the two structural domains making the active site (underlined) and amino acids involved in the enzymatic reaction (bold). (C) Schematic representation of the active site with the interacting network involving $Mg^{2+}$ ions, NADPH, IpOHA, and water molecules.

rate of 170 $\mu$L/min. To minimize any back exchange, the column and solvents were cooled in an ice bath. Direct mass measurement of the deuterated peptides was obtained by diverting one-eighth of the column flow to the mass spectrometer.

*Sequence Assignments.* Nondeuterated isomeroreductase was digested using the same experimental conditions that were used for the H−D exchange studies described above. Peptic peptides were separated on a Brownlee (Perkin-Elmer) $C_8$ reversed phase column (2.1 mm × 100 mm) using a linear gradient from 16 to 64% acetonitrile over the course of 25 min at a flow rate of 200 $\mu$L/min. Mass spectra were acquired by diverting one-eighth of the flow to the mass spectrometer. Collected fractions, containing generally from three to eight fragments, were dried and submitted to Edman degradation analysis.

The N-terminal sequences of peptic peptides of acetohydroxy acid isomeroreductase were determined by 10 Edman degradation cycles. Automated Edman degradation was performed by using an Applied Biosystems model 477A protein sequencer, and amino acid phenylthiohydantoin derivatives were identified and quantitated on line with a model 120A HPLC system (Applied Biosystems), as recommended by the manufacturer. Additional sequence information for some peptides was obtained by tandem mass spectrometry using an in-house-built nanospray source, according to a previously described method (*20*). No major difference was found in the digestion profiles of the free enzyme and of the complexes. For this reason, it was not necessary to sequence the peptic peptides from the complexes.

*Crystallographic Structure*. Results were analyzed at the molecular level using the crystallographic PDB file deposited in the Brookhaven Protein Data Bank under file name 1YVE (*1*). In our convention, the residue numbering includes the signal peptide. Thus, the first residue of the mature protein is V73. See Swiss-Prot entry ILV5-SPIOL.

## RESULTS

*H−D Exchange Mapping of Peptic Peptides*. After the preliminary step of identification of the peptic fragments using the combination of Edman degradation and MS, the H−D exchange method was optimized in terms of rapidity, sensitivity, and reproducibility. Then H−D exchange experiments were carried out to study the influence of ligands ($Mg^{2+}$, NADPH, and IpOHA) on the structure and dynamics of isomeroreductase. Deuterium levels are given in Tables 1−4 for the peptides that exhibited decreased or increased levels of deuterium with respect to the free enzyme. Thus, regions with decreases in mass are more shielded from solvent and consequently more structured, whereas those with increases in mass are more accessible to the solvent and more mobile.

We previously ensured by H−D exchange kinetics and global H−D measurements that after incubation for 3 h in $D_2O$, the H−D exchange rates were sufficiently different between the different complexes and the free enzyme. Consequently, we were able to detect the conformational changes linked to the binding of the ligands (data not shown). The usual procedure for studying conformational changes using isotope exchange requires the kinetic analyses of deuterium incorporation for each peptide. In the case of isomeroreductase, as the mass increases largely exceeded the mass error and vary little after 3 h, and because of the large number of peptides, we chose to study the structural changes at that time. However, it is important to note that the half-lives for H−D exchange of NH within folded proteins span a range of seconds to months. Using 3 h to exchange the NH (see Materials and Methods), we were able to detect exchange of those NH with half-lives near 3 h. Since we chose to detect H−D exchanges only for those NH, we could not detect structural changes in regions where the NH exchange half-lives were very different, either faster or slower. Moreover, since the HPLC step was performed in a protic solvent, deuterium located in the side chains was replaced with hydrogens, leaving deuterium only at peptide amide linkages (*21*).

The following criteria were used to define the threshold above which the mass change was deemed to be significant. On the basis of the mass acquisition step of *m*/*z* 0.2, corresponding to a typical error of 0.4 Da for a doubly charged ion, a variation of ±1 Da was chosen as the minimum mass change reflecting a structural modification. In Tables 1−4, the location of the peptides along the backbone, the corresponding secondary structures, and the role of these regions are given to illustrate the influence of the ligands on structure. For a uniform comparison between peptides of different lengths, we calculated the influence of the ligands for each peptide by dividing the mass change by the total number of exchangeable amide hydrogens. This led us to adopt a color code (Figures 2−5) with which to reflect the different changes in the deuterium levels detected upon binding of the ligands. We chose to use four levels of blue corresponding to changes from 0 to 10%, 10 to 20%, 20 to 40%, and 40 to 60%. The last two ranges were made wider because only few peptides exhibited changes from 20 to 40% and 40 to 60%. This representation was used to illustrate the conformational changes detected for each complex. Furthermore, a view of the three-dimensional structure of the dimer along with the primary sequence of isomeroreductase with indicated secondary structures and regions of importance (regions I−V) is given in panels A and B of Figure 1. A detailed view of the active site is given in Figure 1C (*1*) which better follows the results discussed at the level of active site formation. As mentioned above, it is important to remember that conformational changes observed upon ligand binding are described compared to the free enzyme. More, for obvious interpretations of results, we used the three-dimensional structure of the Ir−$Mg^{2+}$−NADPH−IpOHA complex which, of course, did not reflect the structure of the free enzyme or of the other complexes. Therefore, the use of the crystal structure of this complex is very useful, in particular, in viewing both sides of the enzyme.

*Study of the Ir−$Mg^{2+}$ Complex.* The influence of $Mg^{2+}$ ions on the conformation of isomeroreductase detected by H−D exchange and ESI-MS experiments is shown in Table 1 and Figure 2. As expected from biochemical and structural data, the segment which enclosed region IV corresponding to the binding site of $Mg^{2+}$ 2 was found to be less accessible to the deuterated solvent (decreases in mass) in the presence of this cation. In contrast, region III which corresponds to the binding site of both $Mg^{2+}$ 1 and $Mg^{2+}$ 2 did not exhibit any conformational modification. Decreases in mass were found for the C-terminal domain in regions near or at the interface of N- and C-terminal domains forming the active site (A23, A24, A29, and the C-terminus). Interestingly, decreases in mass were also observed in the N-terminal domain for peptides belonging to the active site (B8−A9, A10, and loop B5). Similarly, a fragment including α-helix A2, which belongs to region I involved in NADPH binding, was found to be more protected against solvent exchange. A small degree of deuterium incorporation change was found at the dimer interface with segments involved in α-helices A17 and A18. In marked contrast, a large decrease in mass was observed for the dimer loop upon $Mg^{2+}$ ions binding.

*Study of the Ir−NADPH Complex.* The influence of NADPH on the conformation of isomeroreductase is summarized in Table 2 and depicted in Figure 3. We showed

Table 1: Localization of Segments with Mass Changes Reflecting Structural Modifications upon Binding of $Mg^{2+}$ Ions[a]

| residues | secondary structure | mass change $\Delta(\Delta m)$ (Da) | accessibility change (%) | comments |
|---|---|---|---|---|
| 128−151 | A2 | −4.8 | −21 | region I |
| 156−168 | loop and B5 | −4.1 | −34 | N−C |
| 247−258 | B8 loop−beginning of A9 | −1.1 | −12 | region II, N−C, AA* |
| 256−267 | A9 | −2.9 | −29 | region II, N−C |
| 280−297 | A10 | −1.0 | −6 | structural role |
| 403−422 | end A17−A18 | −1.0 | −5 | dimer interface with N−C |
| 423−431 | dimer loop | −3.5 | −50 | dimer interface |
| 465−484 | A20 | −3.3 | −17 | structural role |
| 479−492 | end A20−A21 | −1.3 | −10 | dimer interface, N−C, AA*, region IV |
| 498−505 | A23 | −1.5 | −21 | N−C, AA* |
| 510−519 | A24 | −2.0 | −25 | N−C, region V, AA* |
| 559−570 | A29 | −1.9 | −19 | N−C |
| 581−589 | C-terminus | −2.0 | −28 | N−C |

[a] N−C represents the N−C interface domain. AA* represents the segment containing amino acids involved in the active site. The change of accessibility of the deuterated solvent is calculated by dividing the mass change $\Delta(\Delta m)$ by the total number of exchangeable amide hydrogens of each peptic peptide.

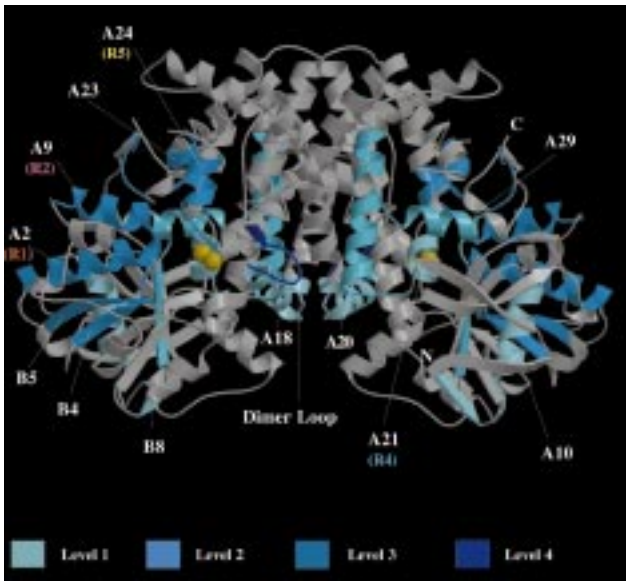


FIGURE 2: Influence of $Mg^{2+}$ ions on the conformation of isomeroreductase visualized by H−D exchange mapping of peptic peptides. Blue regions correspond to a decrease in the level of deuterium incorporation upon Mg binding. The binding of $Mg^{2+}$ ions led to primary structuring of the active site as shown by the structuring of regions at the interface of the two structural domains. The graded shades of blue reflect the different levels of conformational change from small (light blue) to large (dark blue). For identification of conserved regions of acetohydroxy acid isomeroreductase, see the crystal structure complexed with NADPH−$Mg^{2+}$−IpOHA (Figure 1A).

that the binding of NADPH led to a mass decrease in the N-terminal domain consistent with reduced access to solvent at the level of regions I and II involved in the binding of this ligand (α-helices and $\beta$-strand A1−B4−A2 and α-helix A9). Interestingly, changes in the deuterium accessibility were found for a large part of the open twisted $\alpha/\beta$ Rossman fold structure with segments including A7−B7−A8−B8 secondary structural elements. Regions of the N-terminal domain at the interface of the two domains were also found to be less exposed to solvent upon NADPH binding (part of A9 and B9). It is noteworthy that decreases in mass also occurred in the C-terminal domain which was distant from the NADPH binding site, notably with fragments including α-helices A12, A13−A15, A20−A21, A22−A23−beginning of A24, and the C-terminus. Another feature of the NADPH influence is the further decrease in mass observed at the dimer interface, including α-helices A17 and A18. As observed with $Mg^{2+}$ ions, the binding of NADPH also induces a large decrease in mass in the dimer loop.

*Study of the Ir−$Mg^{2+}$−NADPH Complex.* Results of the influence of both $Mg^{2+}$ ions and NADPH on the conformation of isomeroreductase are presented in Table 3 and Figure 4. Compared with the binding of $Mg^{2+}$ ions and NADPH alone, the combination of these two cofactors led on one hand to larger decreases in mass and on the other hand to additional peptides with mass changes.

Decreases in mass found in the N-terminal domain correspond to segments at the interface of the two domains (A8−B8 and A9) and to segments including region I (A1−B4−A2) and region II (A9) interacting with NADPH. All other segments having decreases in mass consistent with a reduced access to the deuterated solvent correspond to structural regions (N-terminus, A4, B9, and A11). Only α-helix A5 in the N-terminal domain was found to exhibit an increase in solvent access. With regard to the C-terminal domain, binding of $Mg^{2+}$ ions and NADPH led to a large decrease in the accessibility of the deuterated solvent in regions at the interface of the two domains (part of A18, part of A20−A21, A24, and the C-terminus). Additional structural segments, including α-helices A13−A14−A15, A20, A26, and the C-terminus, were also found to be shielded from solvent. Both regions III (A11) and IV (A24) involved in the binding of $Mg^{2+}$ 1 and $Mg^{2+}$ 2, respectively, were found to have decreased masses, whereas only region IV was found to be involved in conformational changes for the complexes with $Mg^{2+}$ ions or NADPH alone. In addition, segments corresponding to region V (A25−A26) were found to be less exposed to the deuterated solvent. Similar to the Ir−$Mg^{2+}$ and Ir−NADPH complexes, a small degree of deuterium incorporation was found at the dimer interface (A17−A18), and large decrease in mass was still observed for the dimer loop. Increases in the extent of deuterium incorporation were found only for segments corresponding to the end of α-helix A25 (end of region V) and to the beginning of α-helix A26 at the interface of the two domains.

*Study of the Ir−$Mg^{2+}$−NADPH−IpOHA Complex.* Conformational changes involved upon IpOHA binding are summarized in Table 4 and depicted in Figure 5. The binding of this competitive inhibitor was found to further decrease the solvent accessibility of the overall structure of the dimer of isomeroreductase compared to the results of H−D exchange in the Ir−$Mg^{2+}$−NADPH complex. As IpOHA binds to the C-terminal domain, important conformational modifications in this domain were observed. A segment corresponding to region IV (α-helices A20 and A21) was found to be protected to a similar degree against H−D exchange compared with the Ir−$Mg^{2+}$−NADPH complex, whereas surprisingly, region III had the same deuterium content as the free enzyme. Regions of the C-terminal domain at the interface of the two domains were also found to have reduced deuterium levels (part of A18, part of A20, A21, A22−A23, and the C-terminus). Other regions which cor-

Table 2: Localization of Segments with Mass Changes Reflecting Structural Modifications upon Binding of NADPH[a]

| residues | secondary structure | mass change $\Delta(\Delta m)$ (Da) | accessibility change (%) | comments |
|---|---|---|---|---|
| 116−133 | A1−B4 | −2.7 | −18 | region I |
| 128−151 | B4−A2 | −2.0 | −8 | region I |
| 209−227 | A7−B7 | −5.9 | −35 | AA* |
| 229−254 | A8−B8 | −5.4 | −23 | N−C, AA* |
| 256−267 | A9 | −1.3 | −13 | region II, N−C |
| 262−274 | B9 | −1.1 | −9 | region II, close to N−C |
| 324−332 | A12 | −2.2 | −27 | end of region III |
| 346−362 | A13−A14−A15 | −1.4 | −10 | structural role |
| 403−422 | end of A17−A18 | −2.9 | −15 | dimer interface, N−C |
| 423−431 | dimer loop | −4.0 | −57 | dimer interface |
| 454−471 | loop−A20 | −1.7 | −10 | structural role |
| 465−484 | A20 | −1.7 | −9 | dimer interface |
| 479−492 | end of A20−A21 | −1.7 | −14 | dimer and N−C interfaces, AA*, region IV |
| 497−512 | loop with A22−A23− beginning of A24 | −2.9 | −19 | downstream of region V, N−C, AA* |
| 581−589 | C-terminus | −1.7 | −21 | N−C |

[a] N−C represents the N−C interface domain. AA* represents the segment containing amino acids involved in the active site. The change of accessibility of the deuterated solvent is calculated by dividing the mass change $\Delta(\Delta m)$ by the total number of exchangeable amide hydrogens of each peptic peptide.

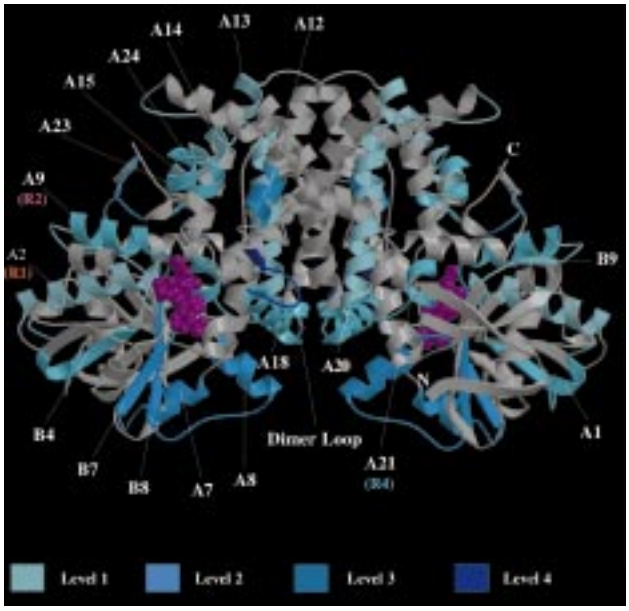


FIGURE 3: Influence of NADPH on the conformation of isomeroreductase visualized by H−D exchange mapping of peptic peptides. Blue regions correspond to a decrease in the level of deuterium incorporation upon NADPH binding. Binding of NADPH leads to a decrease in the accessibility of the N-terminal domain toward the deuterated solvent. Interestingly, binding of NADPH also led to the buildup of a few segments in the C-terminal domain around or in the active site. The graded shades of blue reflect the different levels of conformational changes from small (light blue) to large (dark blue). For identification of conserved regions of acetohydroxy acid isomeroreductase, see the crystal structure complexed with NADPH−$Mg^{2+}$−IpOHA (Figure 1A) (*1*).

respond to secondary structures such as α-helices A13−A14−A15 and A28 were also found to be shielded from the deuterated solvent. A distant reduced level of deuterium incorporation in the N-terminal domain was also found for peptides making a large part of the α/*β* Rossman fold structure. These regions included region I (B3−A1−B4−A2) and region II (end of the A9 loop) interacting with NADPH, which also help to form the active site at the interface of the two domains (B5, A7−B7, and A8−B8), or remotely (B2 and A5). Like the case for the $Mg^{2+}$−NADPH complex, an increase in mass was found in the N-terminal domain for α-helix A5. An increase in deuterium level was observed for *β*-strand B2 only in the complex with IpOHA.

## DISCUSSION

With a view of better characterizing the conformational influence of the ligands, we performed experiments using isotopic exchange and MS with peptides according to a procedure described by Zhang and Smith (*9*), adapted for our ESI-MS method. In a first step, the peptic digestion was optimized and most of the fragments were identified using both ESI-MS and Edman degradation after an HPLC separation of digested fragments.

### *Sequence Assignment*

To limit the back exchange of the deuterated peptides, proteolysis was carried out with pepsin which is active at low pH and low temperature. If a specific protease, like trypsin, could have been used, the identification of the peptides could have been carried out using only MS. Because of the use of a protease with a low specificity (pepsin), N-terminal sequencing combined with accurate mass measurement was needed to identify all the peptides. For Edman degradation analyses, data were collected for 10 cycles and results were read according to the concentration of each PTH amino acid linked to peptide concentration. Using MS data and the N-terminal sequences obtained by Edman degradation, we were able to accurately identify most of the peptic fragments and to confirm the charge state of the ions. In comparison with MS−MS sequencing where peptic fragments show limited charge fragmentation, the direct sequencing of peptic peptides is easier to carry out. In the case of fragments that were not identified by Edman degradation due to their low concentration, collision-induced dissociation (CID) spectra were acquired using an in-house-built nanospray ion source. This allowed optimization of the fragmentation parameters and acquisition of the signal for a long time which improved the signal-to-noise ratio. Mass spectrometry sequencing was used for only few peptides which belonged to particularly important regions (e.g., residues 479−492).

Thus, using the complementarity of Edman degradation and mass spectrometry, 93% of the 593 residues comprising the primary sequence of the plant enzyme were covered. Missing fragments were found to be small peptides presumed to elute with salts at the beginning of the separation by HPLC. Fortunately, these segments were not essential since they did not include regions involved in the binding of ligands or regions located at the interface of the two domains forming the active site. Overall, combined Edman degradation and LC−ESI-MS data allowed the determination of the sequences, the masses, the charge states, and retention times of most of the peptic peptides. This led to the creation of a database, which proved to be very useful for peptide identification and interpretation of the results from H−D exchange experiments. H−D exchange mapping of the peptic

Table 3: Localization of Segments with Mass Changes Reflecting Structural Modifications upon Binding of $Mg^{2+}$ Ions and NADPH[a]

| residues | secondary structure | mass change $\Delta(\Delta m)$ (Da) | accessibility change (%) | comments |
|---|---|---|---|---|
| 72−86 | N-terminus | −1.5 | −14 | − |
| 115−128 | A1−loop | −1.8 | −14 | region I |
| 128−151 | B4−A2 | −2.0 | −8 | region I |
| 177−186 | A4 | −1.7 | −19 | structural role |
| 187−194 | A5 | 1.5 | +21 | structural role |
| 223−254 | A8−B8 | −6.1 | −20 | N−C, AA* |
| 256−267 | A9 | −1.7 | −17 | region II, N−C |
| 262−274 | B9−loop | −2.3 | −19 | region II, close to N−C |
| 312−316 | A11 | −1.5 | −37 | region III |
| 346−362 | A13−A14−A15 | −1.8 | −13 | structural role |
| 403−422 | end of A17−A18 | −1.9 | −10 | dimer interface, N−C |
| 423−431 | dimer loop | −3.6 | −51 | dimer interface |
| 454−471 | A20 | −2.4 | −14 | structural role |
| 479−492 | A20−A21 | −2.9 | −22 | dimer interface, N−C, AA*, region IV |
| 510−519 | A24 | −2.0 | −25 | N−C, region V, AA* |
| 524−532 | A25−A26 | 2.0 | 28 | dimer interface, region V |
| 542−554 | A27−A28 | −1.7 | −15 | dimer interface |
| 571−578 | C-terminus | −1.0 | −17 | N−C |
| 579−586 | C-terminus | −1.1 | −16 | N−C |
| 588−593 | C-terminus | −2.2 | −55 | N−C |

[a] N−C represents the N−C interface domain. AA* represents the segment containing amino acids involved in the active site. The change of accessibility of the deuterated solvent is calculated by dividing the mass change $\Delta(\Delta m)$ by the total number of exchangeable amide hydrogens of each peptic peptide.

peptides for the free enzyme and complexes of isomeroreductase with $Mg^{2+}$, NADPH, $Mg^{2+}$−NADPH, and NADPH−$Mg^{2+}$−IpOHA was performed. Comparison of the deuterium content of the peptic peptides between the free enzyme and complexes allowed the characterization of the influence of Mg ions, NADPH, and IpOHA. However, it is important to note that the crystallographic structure used to discuss the results referred to the whole complex (Ir−NADPH−$Mg^{2+}$−IpOHA). Results are discussed according to the "local unfolding model" proposed by Hvidt (*22*) and promoted by Englander (*23*).

### *H−D Exchange Mapping of Peptic Peptides*

*Role of $Mg^{2+}$ Ions (Figure 2).* The binding and the function of the cations are particularly important. First, $Mg^{2+}$ is essential for the two-step reaction catalyzed by isomeroreductase. Second, the averaged $k_d$ and $K_m$ values of isomeroreductase for $Mg^{2+}$ ions are 5 and 6 $\mu$M, respectively (*2*). When the strong affinity of the enzyme for these cations and the important electrostatic interaction between $Mg^{2+}$ ions and neighboring amino acids (D315, E319, and E492) are considered, $Mg^{2+}$ ions could be expected to trigger some conformational modifications, especially in regions III and IV. Indeed, we clearly demonstrated that $Mg^{2+}$ ion binding is important in restructuring the active site, illustrated by the large decrease in the extent of deuterium incorporation. Interestingly, region III, involved in the binding of the two cations, did not show any deuterium incorporation change upon $Mg^{2+}$ ions binding, indicating no conformational modification. In contrast, in region IV, the binding site of $Mg^{2+}$ 2 was found to be structured upon binding of this cation. This result could be explained by the number of electrostatic interactions involving $Mg^{2+}$ 1, compared with $Mg^{2+}$ 2, and/or by the fact that $Mg^{2+}$ 1 binds to only one

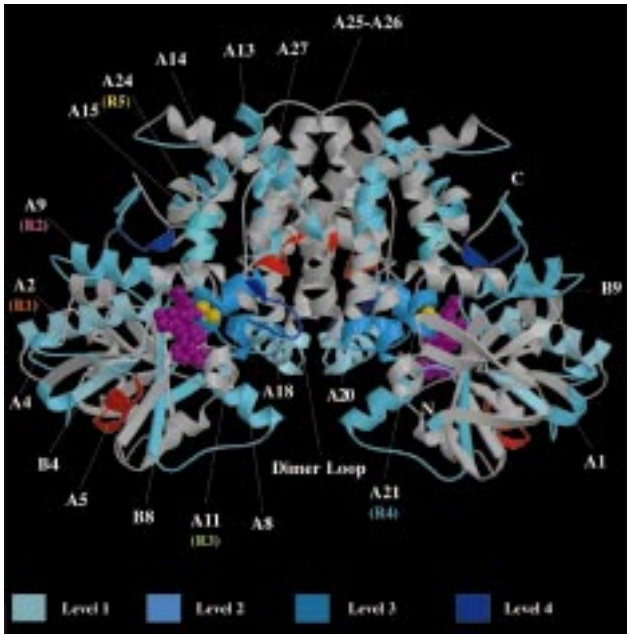


FIGURE 4: Influence of $Mg^{2+}$ and NADPH on the conformation of isomeroreductase visualized by H−D exchange mapping of peptic peptides. Blue or red segments correspond to a decrease or an increase in the level of deuterium incorporation upon binding of $Mg^{2+}$ or NADPH, respectively. Results showed that in the presence of these two cofactors the structuring is enhanced at the interface of the two domains and in the N- and C-terminal domains involved in the binding of NADPH and $Mg^{2+}$ ions, respectively. These cofactors led to a strong protection of the active site along with an opening of the active site for inhibitor (substrate) binding. The graded shades of blue reflect the different levels of conformational changes from small (light blue) to large (dark blue). For identification of conserved regions of acetohydroxy acid isomeroreductase, see the crystal structure complexed with NADPH−$Mg^{2+}$−IpOHA (Figure 1A) (*1*).

secondary structural unit (A11), whereas $Mg^{2+}$ 2 bridges three secondary structures (A11, B8, and A21). This means that part of the electrostatic network involving amino acids interacting with $Mg^{2+}$ 2 may be formed at an early stage and plays an important role in the active site buildup. $Mg^{2+}$ ions also led to a remote action at the N−C domain interface in the N-terminal domain. This long-range buildup of both domains was assigned to a structural ordering of regions forming the active site. As mentioned above, $Mg^{2+}$ ions were also found to influence the dimer interface interactions. The dimer loop was found to play an important role in dimer stability with a marked decrease in mass after $Mg^{2+}$ ion binding. The role of this dimer loop for each binding ligand will be discussed in a separate paragraph.

*Role of NADPH (Figure 3).* According to the X-ray diffraction data (*1*), NADPH binds in the N-terminal domain composed of a typical $\alpha/\beta$ Rossman fold structure. The nucleotide binding site (residues 127−251) is formed by the five outer strands (B5−B4−B6−B7−B8) with the $\beta-\alpha-\beta$ motif (B4−A2−B5) which is a canonical diphosphate-binding motif (*24*). The tight binding of the cofactor in this domain involved H-bonds with residues G132, G134, Q136, Q143, and D146 of region I (132−147) and residues G255, V258, R259, and G265 of region II (255−268). Electrostatic contacts with the phosphate groups involving R162, S165, and S167 (strand B5 and helix A3) also contribute to the strong stabilization of NADPH. This coenzyme is shielded

Table 4: Localization of Segments with Mass Changes Reflecting Structural Modifications upon Binding of $Mg^{2+}$ Ions, NADPH, and IpOHA[a]

| residues | secondary structure | mass change $\Delta(\Delta m)$ (Da) | accessibility change (%) | comments |
|---|---|---|---|---|
| 72−86 | N-terminus, B1 | −3.9 | −35 | − |
| 93−100 | B2 | 1.5 | 21 | structural role |
| 107−115 | B3−loop | −1.3 | −16 | region I |
| 115−128 | A1−loop | −4.2 | −32 | region I |
| 128−151 | B4−A2 | −5.2 | −23 | region I |
| 156−168 | B5 | −2.6 | −22 | N−C |
| 187−194 | A5 | 2.0 | 28 | structural role |
| 209−227 | A7−B7 | −1.4 | −8 | AA* |
| 223−254 | A8−B8 | −7.9 | −25 | N−C |
| 262−274 | end of A9−loop | −2.1 | −17 | region II, N−C |
| 346−362 | A13−A14−A15 | −1.8 | −13 | structural role |
| 403−422 | end of A17−A18 | −1.9 | −10 | dimer interface, N−C |
| 423−431 | dimer loop | −3.7 | −53 | dimer interface |
| 451−467 | loop−A20 | −5.0 | −31 | structural role |
| 465−484 | A20 | −3.5 | −18 | structural role |
| 479−492 | end of A20−A21 | −1.9 | −15 | dimer interface, N−C, AA*, region IV |
| 497−512 | A22−A23 | −3.8 | −25 | N−C, AA* |
| 545−554 | A28 | −1.8 | −22 | structural role |
| 571−578 | C-terminus | −1.1 | −18 | N−C |
| 579−586 | C-terminus | −1.0 | −14 | N−C |
| 581−589 | C-terminus | −4.1 | −58 | N−C |
| 588−593 | C-terminus | −2.2 | −55 | N−C |

[a] N−C represents the N−C interface domain. AA* represents the segment containing amino acids involved in the active site. The change of accessibility of the deuterated solvent is calculated by dividing the mass change $\Delta(\Delta m)$ by the total number of exchangeable amide hydrogens of each peptic peptide.

from the solvent in the protein core, with only the adenine moiety of NADPH on the surface of the protein.

As expected from the structure (*1*), the binding of NADPH led to a change in deuterated solvent accessibility of regions I and II interacting with this cofactor. These results are consistent with the occurrence of H-bond formation involving residues of regions I and II, leading to the binding of NADPH to isomeroreductase. Binding of NADPH in the N-terminal domain structured not only regions I and II, which directly interact with this cofactor, but also a large part of the $\alpha/\beta$ Rossman fold structure. This would structure regions at the interface of the two domains making the active site. As observed with $Mg^{2+}$ ions, the binding of NADPH also induces a remote buildup of the C-terminal domain, as seen with decrease in mass detected in regions of the C-terminal domain at the N−C domain interface. As shown for $Mg^{2+}$ ions, this would suggest a long-range structural effect of the two domains by reinforcing the cohesion of the N−C domain interface. This last result is also illustrated by still weaker deuterium level incorporation in the segment associated with the binding site of the $Mg^{2+}$ 2 (region IV) after the binding of NADPH. In contrast, region III was still found to be highly protected from solvent. These results clearly demonstrated that NADPH is a major factor in forming the N-terminal domain and the active site, deeply buried inside the protein core. This is in agreement with a general role of NADPH in the formation of the active site, as Wang et al. (*19*, *25*) demonstrated the same structural effect of this cofactor binding to *E. coli* dihydropicolinate reductase enzyme, and to *Clostridium glutanicum* diaminopimelate dehydrogenase.

*Role of $Mg^{2+}$ Ions and NADPH (Figure 4).* Detected conformational changes for the Ir−$Mg^{2+}$−NADPH complex

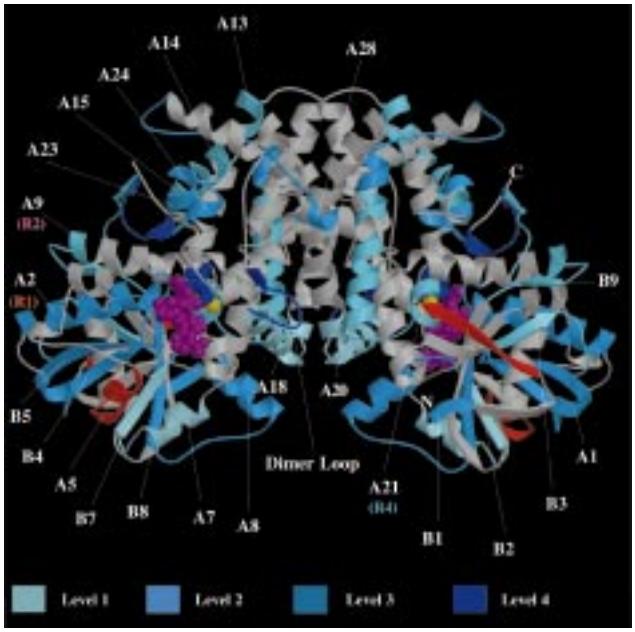


FIGURE 5: Influence of $Mg^{2+}$, NADPH, and IpOHA on the conformation of isomeroreductase visualized by H−D exchange mapping of peptic peptides. Blue or red segments correspond to a decrease or an increase in the level of deuterium incorporation upon IpOHA binding, respectively. Comparing the conformational differences between Ir−$Mg^{2+}$−NADPH and Ir−NADPH−$Mg^{2+}$−IpOHA, we showed that in the presence of the competitive inhibitor the protection of the C-terminal domain, involved in the binding of IpOHA, is enhanced toward solvent penetration. However, the main influence of these inhibitor occurred in the N-terminal domain, leading to a large buildup of the active site. The graded shades of blue reflect the different levels of conformational changes from small (light blue) to large (dark blue). For identification of conserved regions of acetohydroxy acid isomeroreductase, see the crystal structure complexed with NADPH−$Mg^{2+}$−IpOHA (Figure 1A) (*1*).

were nearly a simple addition of those for the Ir−$Mg^{2+}$ and Ir−NADPH complexes with variations in terms of length and intensities of structured segments. Moreover, additional segments with decreased masses were found. For the N-terminal domain, further decreases in mass were found for the N-terminus and α-helix A4. Increased structuring occurred for regions I and II which interact with NADPH. For the C-terminal domain, this higher degree of structure is illustrated with the appearance of a decrease in mass for region III, region V, and the C-terminus. These additional decreases in mass, together with those already existing at the N−C domain interface, indicate a high level of structure in the protein core. These results are consistent with the active site structuring prior to substrate (or inhibitor) binding, and explain the ordered mechanism of ligand binding in terms of structural changes. Indeed, the enzyme-catalyzed reaction obeys an ordered mechanism in which NADPH and $Mg^{2+}$ ions bind first and independently, followed by substrate or inhibitor binding (*2*). No mass change was observed for the $Mg^{2+}$ 1 binding site in region III upon independent binding of $Mg^{2+}$ and NADPH. However, the combined binding of both $Mg^{2+}$ and NADPH triggers a mass decrease in this region, which can be explained by a cooperative action for structuring the active site. According to the X-ray structure, the buildup of region III may be explained by the occurrence of an electrostatic network, involving NADPH, $Mg^{2+}$ 1, and water molecule(s) as shown in Figure 1C (*1*). Region IV was also found to be more structured upon binding of $Mg^{2+}$

ions and NADPH than in Ir−Mg and Ir−NADPH complexes alone. Consequently, NADPH binding would have a role in the cooperative ordering of regions III and IV via this electrostatic network. These results clearly show that the electrostatic network involving the NADPH, the two $Mg^{2+}$ ions, and water molecules (*1*) is partially formed after the fixation of $Mg^{2+}$ ions and NADPH. This network may play an important role in the formation of the active site, for substrate (or inhibitor) binding. The change of the enzyme structure after the binding of $Mg^{2+}$ ions and NADPH led to a decrease in solvent accessibility in many regions and to a small increase in the extent of solvent exposure for α-helix A5 in the N-terminal domain and α-helices A25 and A26 in the C-terminal domain.

*Role of IpOHA (Figure 5)*. IpOHA is a transition state analogue which behaves as a competitive inhibitor of the plant isomeroreductase. It was shown that this compound exhibits tight binding to the enzyme, resulting in a nearly irreversible inhibition (*5*, *26*). X-ray diffraction data recently provided a detailed view of the active site and provided insight about the reasons for this tight binding. In this model, IpOHA was found to be completely buried inside the active site and held in place via an important network of H-bonds, electrostatic interactions, and hydrophobic contacts (Figure 1C) (*1*).

H−D exchange experiments performed on the whole complex showed an overall conformational change of the plant enzyme, compared to the free enzyme. However, it is more interesting to compare the structural changes of the whole complex with those of the Ir−$Mg^{2+}$−NADPH complex which is the real intermediate of the ligand binding process. Regions already structured in the Ir−$Mg^{2+}$−NADPH complex were found to be further shielded from solvent after IpOHA binding. This additional increase is visualized both through broadening of the protected regions and through a further decrease in the level of deuterium incorporation. As IpOHA binds to the C-terminal domain, large changes were expected in this domain. Unpredictably, the most important decreases in mass were found in the N-terminal domain. A significant decrease in mass was found for a large part of the α/*β* Rossman fold. Surprisingly, conformational changes observed after the binding of IpOHA on the C-terminal domain did not lead to further decreases in mass of regions II, III, and V as compared with the Ir−$Mg^{2+}$−NADPH complex. Indeed, these regions were found to be more accessible to the solvent, in the presence of the competitive inhibitor, than before its binding. This result is consistent with NADPH fluorescence experiments which have shown that after IpOHA binding the emitted fluorescence was decreased to the level of the free NADPH fluorescence. This is in agreement with a change in the relative positions of the regions making the active site. This result may be explained by the tight interaction network in the active site involving IpOHA. Indeed, structural data showed that this network involving the conserved residues of the active site, $Mg^{2+}$ ions, NADPH, IpOHA, and water molecules was very tight. Consequently, binding of this competitive inhibitor led to a large buildup of secondary and tertiary structures around it (*1*, *5*). Therefore, the importance of IpOHA in structuring the active site may explain why it was possible to crystallize the enzyme in the presence of $Mg^{2+}$ ions and IpOHA (R. Dumas and V. Biou, unpublished results), whereas it was impossible to obtain diffraction-quality crystals of the free enzyme or the enzyme complexed with $Mg^{2+}$ ions or NADPH. The nearly irreversible character of IpOHA could therefore be explained by the formation of this highly stable network. Besides the large buildup of isomeroreductase structure upon IpOHA binding, some regions were found to be more accessible to the solvent. This concerned only segments localized in the N-terminal domain and correspond to *β*-strand B2 and α-helix A5. According to the literature, these mass increases could be attributed to compensatory effects after ligand binding (*27*).

*Role of the Dimer*. Our results clearly demonstrated that ligand binding induced conformational changes at the level of both the active site and the dimer interface. In particular, the deuterium accessibility of the dimer loop that extends out toward the other monomer is greatly affected upon ligand binding as $Mg^{2+}$ ions and NADPH alone, together, or complexed with IpOHA induced a mass decrease of about 50%. This result is also in agreement with X-ray diffraction data, which have shown that the dimer loop accounts for 25% of the dimer interface interactions (*1*). Buildup of the active site reinforced the interactions of the dimer. These last results suggested that stabilization of the dimer interface and of the active site region at the interface between the N- and C-terminal domains depends on ligand binding. These findings are in complete agreement with the results of site-directed mutagenesis experiments which demonstrated that monomerization of the enzyme after elimination of the dimer loop led to conformational modification at the level of the $Mg^{2+}$ ion binding site (*7*).

## CONCLUSION

We demonstrated that mass spectrometry combined with H−D exchange could give invaluable new information about the conformational changes triggered by ligand binding ($Mg^{2+}$ ions, NADPH, and IpOHA) on a large protein (114 kDa) such as acetohydroxy acid isomeroreductase. This is, to our knowledge, the first report of an H−D exchange study with such a high-molecular mass biological complex. The results obtained for each complex represent "snapshots" of the conformation of the enzyme for each step of the ordered ligand binding process, providing a "view of the dynamics" of the ligand binding process. These results are a good illustration of the theory of "induced fit" proposed by Khosland (*28*, *29*) in which the binding of a substrate or a cofactor led to a conformational change prior enzymatic reaction.

The important conformational modifications upon ligand binding are in agreement with biochemical studies which show that binding of $Mg^{2+}$ ions and NADPH are required prior to binding of the competitive inhibitor (substrate). This has been interpreted as a cooperative ordering of regions at the N−C domain interface making the active site. IpOHA was found to strongly order regions around it, leading to strong interactions of regions at the edge of the active site. This is in agreement with its tight binding. This result would also account for the nearly irreversible character of this competitive inhibitor.

## ACKNOWLEDGMENT

We thank David Smith, Andrew Mundt, Georges Freyssinet, and Marc Vuilhorgne for helpful discussions.

## REFERENCES


1. Biou, V., Dumas, R., Cohen-Addad, C., Douce, R., Job, D., and Pebay-Peyroula, E. (1997) *EMBO J. 16*, 3405−3415.
2. Dumas, R., Butikofer, M.-C., Job, D., and Douce, R. (1995) *Biochemistry 34*, 6026−6036.
3. Dumas, R., Job, D., Ortholand, J. Y., Emeric, G., Greiner, A., and Douce, R. (1992) *Biochem. J. 288*, 865−874.
4. Chunduru, S. K., Mrachko, G. T., and Calvo, K. C. (1989) *Biochemistry 28*, 486−493.
5. Dumas, R., Cornillon-Bertrand, C., Guigue-Talet, P., Genix, P., Douce, R., and Job, D. (1994) *Biochem. J. 301*, 813−820.
6. Dumas, R., Lebrun, M., and Douce, R. (1991) *Biochem. J. 277*, 469−475.
7. Wessel, P. M., Biou, V., Douce, R., and Dumas, R. (1998) *Biochemistry 37*, 12753−12760.
8. Smith, D. L., and Zhang, Z. (1994) *Mass Spectrom. Rev. 13*, 411−429.
9. Zhang, Z., and Smith, D. L. (1993) *Protein Sci. 2*, 522−531.
10. Wagner, D. S., and Anderegg, R. J. (1994) *Anal. Chem. 66*, 706−711.
11. Wang, F., and Tang, X. (1996) *Biochemistry 35*, 4069−4078.
12. Johnson, R. S., and Walsh, K. A. (1994) *Protein Sci. 5*, 2411−2418.
13. Miranker, A., Robinson, C. V., Radford, S. E., Aplin, R. T., and Dobson, C. M. (1993) *Science 262*, 896−900.
14. Dharmasiri, K., and Smith, D. L. (1996) *Anal. Chem. 68*, 2340−2344.
15. Grob, M., Robinson, C. V., Mayhew, M., Hartl, F. U., and Radford, S. E. (1996) *Protein Sci. 5*, 2506−2513.
16. Zhang, Z., Post, C. B., and Smith, D. L. (1996) *Biochemistry 35*, 779−791.
17. Guy, P., Remigy, H., Jaquinod, M., Bersch, B., Blanchard, L., Dolla, A., and Forest, E. (1996) *Biochem. Biophys. Res. Commun. 218*, 97−103.
18. Anderegg, R. J., and Wagner, D. S. (1995) *J. Am. Chem. Soc. 117*, 1374−1377.
19. Wang, F., Blanchard, J. S., and Tang, X. J. (1997) *Biochemistry 36*, 3755−3759.
20. Wilm, M., and Mann, M. (1996) *Anal. Chem. 68*, 1−8.
21. Smith, D. L., Deng, Y., and Zhang, Z. (1997) *J. Mass Spectrom. 32*, 135−146.
22. Hvidt, A., and Nielsen, S. O. (1966) *Adv. Protein Chem. 21*, 287−386.
23. Englander, S. W., Calhoun, D. B., Englander, J. J., Kallenbach, R. K., Liem, H., Malin, E. L., Mandal, C., and Rogero, J. R. (1980) *Biophys. J. 32*, 577−587.
24. Branden, C. I., and Tooze, J. (1991) *Introduction to protein structure*, Garland Publishing Inc., New York.
25. Wang, F., Scapin, G., Blanchard, J. S., and Hogue Angeletti, R. (1998) *Protein Sci. 7*, 293−299.
26. Dumas, R., Vives, F., Job, D., Douce, R., Biou, V., Pebay-Peroula, E., and Cohen-Addad, C. (1995) *Brighton Crop Prot. Conf.—Weeds*, 833−842.
27. Engen, J. R., Smithgall, T. E., Gmeiner, W. H., and Smith, D. L. (1997) *Biochemistry 36*, 14384−14391.
28. Koshland, D. E. (1968) *Adv. Enzyme Regul. 6*, 291−301.
29. Koshland, D. E., and Neet, K. E. (1968) *Annu. Rev. Biochem. 37*, 359−410.


BI982412E